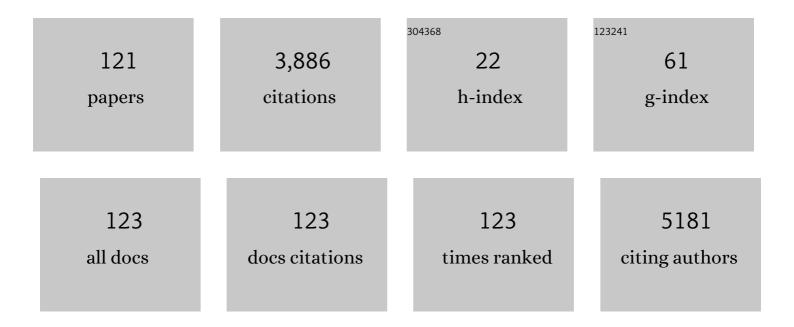
Hyun Cheol Koo

List of Publications by Year in descending order

Source: https://exaly.com/author-pdf/21141/publications.pdf Version: 2024-02-01



#	Article	IF	CITATIONS
1	Room-Temperature Nonreciprocal Charge Transport in an InAs-Based Rashba Channel. ECS Journal of Solid State Science and Technology, 2022, 11, 045011.	0.9	Ο
2	Investigation of magnetic properties of Pt/CoFeB/MgO layers using angle-resolved spin-torque ferromagnetic resonance spectroscopy. Journal of Applied Physics, 2022, 131, .	1.1	2
3	Demonstration of in-plane magnetized stochastic magnetic tunnel junction for binary stochastic neuron. AIP Advances, 2022, 12, .	0.6	4
4	Spin Precession and Spin harge Conversion in a Strong Rashba Channel at Room Temperature. Electronic Materials Letters, 2021, 17, 324-330.	1.0	0
5	Effects of Interfacial Oxidization on Magnetic Damping and Spin–Orbit Torques. ACS Applied Materials & Interfaces, 2021, 13, 19414-19421.	4.0	7
6	Néel-type skyrmions and their current-induced motion in van der Waals ferromagnet-based heterostructures. Physical Review B, 2021, 103, .	1.1	110
7	Effect of the spin-orbit interaction at insulator/ferromagnet interfaces on spin-orbit torques. Physical Review B, 2021, 103, .	1.1	5
8	Theory of spin-torque ferrimagnetic resonance. Physical Review B, 2021, 104, .	1.1	4
9	Surface morphology evolution and underlying defects in homoepitaxial growth of GaAs (110). Journal of Alloys and Compounds, 2021, 874, 159848.	2.8	2
10	Spin-orbit torques induced by spin Hall and spin swapping currents of a separate ferromagnet in a magnetic trilayer. Current Applied Physics, 2021, 29, 54-58.	1.1	1
11	A highly controllable doping technique via interdiffusion between epitaxial germanium layers and GaAs. Surfaces and Interfaces, 2021, 26, 101390.	1.5	Ο
12	Interface Engineering of Magnetic Anisotropy in van der Waals Ferromagnet-based Heterostructures. ACS Nano, 2021, 15, 16395-16403.	7.3	7
13	Direct observation of spin accumulation and spin-orbit torque driven by Rashba-Edelstein effect in an InAs quantum-well layer. Physical Review B, 2021, 104, .	1.1	7
14	Field-like spin–orbit torque induced by bulk Rashba channels in GeTe/NiFe bilayers. NPG Asia Materials, 2021, 13, .	3.8	7
15	Orbital torque in magnetic bilayers. Nature Communications, 2021, 12, 6710.	5.8	69
16	Controlling the Magnetic Anisotropy of the van der Waals Ferromagnet Fe ₃ GeTe ₂ through Hole Doping. Nano Letters, 2020, 20, 95-100.	4.5	118
17	Electrical spin transport in a GaAs (110) channel. Current Applied Physics, 2020, 20, 1295-1298.	1.1	1
18	Spin transport at a Pt/InAs quantum well interface using spin Hall and Rashba effects. Applied Physics Letters, 2020, 117, 042403.	1.5	0

2

#	Article	IF	CITATIONS
19	Rashba Effect in Functional Spintronic Devices. Advanced Materials, 2020, 32, e2002117.	11.1	77
20	Magnetoresistance of a ferromagnet/semiconductor interface with a strong Rashba effect. Thin Solid Films, 2020, 706, 138047.	0.8	1
21	Effect of Rashba interaction at normal metal/insulator interface on spin-orbit torque of ferromagnet/normal metal/insulator trilayers. Current Applied Physics, 2019, 19, 1362-1366.	1.1	4
22	Gate-tunable giant nonreciprocal charge transport in noncentrosymmetric oxide interfaces. Nature Communications, 2019, 10, 4510.	5.8	44
23	Reconfigurable spin logic device using electrochemical potentials. Applied Physics Letters, 2019, 114, 152403.	1.5	2
24	Electrical Observation of the Effective Mass in a Single-Crystal WTe2 Layer. Journal of the Korean Physical Society, 2019, 74, 154-158.	0.3	0
25	Anisotropic magnetoresistance in a Ni81Fe19/SiO2/Ca-Bi2Se3 hybrid structure. Thin Solid Films, 2019, 676, 87-91.	0.8	1
26	Large Magnetoconductance in GaAs Induced by Impact Ionization. Journal of the Korean Physical Society, 2019, 75, 1017-1020.	0.3	0
27	Spin-orbit torques associated with ferrimagnetic order in Pt/GdFeCo/MgO layers. Scientific Reports, 2018, 8, 6017.	1.6	36
28	Current-driven dynamics and inhibition of the skyrmion Hall effect of ferrimagnetic skyrmions in GdFeCo films. Nature Communications, 2018, 9, 959.	5.8	301
29	Multi-terminal spin valve in a strong Rashba channel exhibiting three resistance states. Scientific Reports, 2018, 8, 3397.	1.6	12
30	An InSb-based magnetoresistive biosensor using Fe3O4 nanoparticles. Sensors and Actuators B: Chemical, 2018, 255, 2894-2899.	4.0	8
31	Ferromagnet-Free All-Electric Spin Hall Transistors. Nano Letters, 2018, 18, 7998-8002.	4.5	27
32	Deterministic creation and deletion of a single magnetic skyrmion observed by direct time-resolved X-ray microscopy. Nature Electronics, 2018, 1, 288-296.	13.1	108
33	A possible superconductor-like state at elevated temperatures near metal electrodes in an LaAlO3/SrTiO3 interface. Scientific Reports, 2018, 8, 11558.	1.6	1
34	Spin-Orbit Torque and Magnetic Damping in Tailored Ferromagnetic Bilayers. Physical Review Applied, 2018, 10, .	1.5	12
35	Spin-polarization-induced anisotropic magnetoresistance in a two-dimensional Rashba system. Current Applied Physics, 2017, 17, 513-516.	1.1	8
36	Magnetic property (T Ââ^1⁄4Â300ÂK) originated from InZnP:Ag nano-rods fabricated with noble metal Ag using ion milling method. Journal of Alloys and Compounds, 2017, 704, 552-556.	2.8	1

#	Article	IF	CITATIONS
37	Complementary spin transistor using a quantum well channel. Scientific Reports, 2017, 7, 46671.	1.6	7
38	Spin-orbit torque-driven skyrmion dynamics revealed by time-resolved X-ray microscopy. Nature Communications, 2017, 8, 15573.	5.8	143
39	Large spin accumulation and crystallographic dependence of spin transport in single crystal gallium nitride nanowires. Nature Communications, 2017, 8, 15722.	5.8	28
40	GaSb/InGaAs 2-dimensional hole gas grown on InP substrate for III-V CMOS applications. Current Applied Physics, 2017, 17, 1005-1008.	1.1	2
41	Nonlocal Spin Diffusion Driven by Giant Spin Hall Effect at Oxide Heterointerfaces. Nano Letters, 2017, 17, 36-43.	4.5	37
42	Electrical spin transport in cylindrical silicon nanowires with CoFeB/MgO contacts. Applied Physics Letters, 2017, 111, 062402.	1.5	2
43	Observation of spin dependent electrochemical potentials at room temperature in a quantum well structure. Current Applied Physics, 2017, 17, 1455-1458.	1.1	1
44	Formation and magnetic properties of InFeP:Ag nanorods fabricated with noble metal Ag using an ion milling method. Nanotechnology, 2017, 28, 505702.	1.3	3
45	Ballistic Spin Hall Transistor Using a Heterostructure Channel and Its Application to Logic Devices. Journal of Electronic Materials, 2017, 46, 3894-3898.	1.0	5
46	Spin accumulation at in-situ grown Fe/GaAs(100) Schottky barriers measured using the three- and four-terminal methods. Applied Physics Letters, 2016, 109, 122409.	1.5	4
47	Spin-Orbit Coupling Induced Coercivity Change at a Ferromagnet-Semiconductor Interface. Journal of Nanoscience and Nanotechnology, 2016, 16, 10210-10213.	0.9	0
48	Free-electron creation at the 60 \hat{A}^{o} twin boundary in Bi2Te3. Nature Communications, 2016, 7, 12449.	5.8	59
49	All-electric spin transistor using perpendicular spins. Journal of Magnetism and Magnetic Materials, 2016, 403, 77-80.	1.0	10
50	Crystalline Direction Dependence of Spin Precession Angle and Its Application to Complementary Spin Logic Devices. Journal of Nanoscience and Nanotechnology, 2015, 15, 7518-7521.	0.9	0
51	Spin injection in indium arsenide. Frontiers in Physics, 2015, 3, .	1.0	1
52	Electrical spin injection in modulation-doped GaAs from an in situ grown Fe/MgO layer. Applied Physics Letters, 2015, 107, 102407.	1.5	3
53	Electrical detection of coherent spin precession using the ballistic intrinsic spin Hall effect. Nature Nanotechnology, 2015, 10, 666-670.	15.6	67
54	Conductance Change Induced by the Rashba Effect in the LaAlO ₃ /SrTiO ₃ Interface. Journal of Nanoscience and Nanotechnology, 2015, 15, 8632-8636.	0.9	3

#	Article	IF	CITATIONS
55	Exchange-biased ferromagnetic electrodes and their application to complementary spin transistors. Current Applied Physics, 2015, 15, S32-S35.	1.1	2
56	Spin-Based Complementary Logic Device Using Datta–Das Transistors. IEEE Transactions on Electron Devices, 2015, 62, 3056-3060.	1.6	26
57	Fermi surface distortion induced by interaction between Rashba and Zeeman effects. Journal of Applied Physics, 2015, 117, 17C111.	1.1	2
58	New perspectives for Rashba spin–orbit coupling. Nature Materials, 2015, 14, 871-882.	13.3	1,438
59	Determination of g-factor in a quantum well channel with a strong Rashba effect. Journal of Applied Physics, 2014, 115, 17C702.	1.1	2
60	Spin injection and detection in In _{0.53} Ga _{0.47} As nanomembrane channels transferred onto Si substrates. Applied Physics Express, 2014, 7, 093004.	1.1	3
61	New optical transition, structural, and ferromagnetic properties of InCrP:Zn implanted with Cr. Journal of Luminescence, 2014, 154, 593-596.	1.5	4
62	Gate-Controlled Spin-Orbit Coupling in InAs/InGaAs Quantum Well Structures. Journal of Nanoscience and Nanotechnology, 2014, 14, 5212-5215.	0.9	3
63	Interaction Between Rashba and Zeeman Effects in a Quantum Well Channel. Journal of Nanoscience and Nanotechnology, 2014, 14, 3581-3583.	0.9	0
64	Electrical Detection of the Spin Hall Effects in InAs Quantum Well Structure with Perpendicular Magnetization of [Pd/CoFe] Multilayer. IEEE Transactions on Magnetics, 2014, 50, 1-4.	1.2	0
65	Shubnikov-de Haas Oscillation and Potentiometric Methods for Spin–Orbit Interaction Parameter Measurement in an InAs Quantum Well. IEEE Transactions on Magnetics, 2014, 50, 18-21.	1.2	13
66	Enhanced ferromagnetism by preventing antiferromagnetic MnO2 in InP:Be/Mn/InP:Be triple layers fabricated using molecular beam epitaxy. Current Applied Physics, 2014, 14, 558-562.	1.1	2
67	Electric-Field-Induced Spin Injection Enhancement. Journal of Nanoscience and Nanotechnology, 2014, 14, 7911-7914.	0.9	1
68	Gate voltage control of the Rashba effect in a p-type GaSb quantum well and application in a complementary device. Solid-State Electronics, 2013, 82, 34-37.	0.8	9
69	Gate-Controlled Spin-Orbit Interaction in InAs High-Electron Mobility Transistor Layers Epitaxially Transferred onto Si Substrates. ACS Nano, 2013, 7, 9106-9114.	7.3	12
70	Large spatial distribution of spin accumulation in wide Au channel. Solid-State Electronics, 2013, 89, 72-75.	0.8	2
71	Transport of perpendicular spin in a semiconductor channel via a fully electrical method. Applied Physics Letters, 2013, 102, .	1.5	8
72	Separation of Rashba and Dresselhaus spin-orbit interactions using crystal direction dependent transport measurements. Applied Physics Letters, 2013, 103, .	1.5	34

#	Article	IF	CITATIONS
73	Observation of gate-controlled spin―orbit interaction using a ferromagnetic detector. Journal of Applied Physics, 2012, 111, .	1.1	17
74	Effect of the buffer layer on the magnetic properties in CoFe/Pd multilayers. Journal of the Korean Physical Society, 2012, 61, 1500-1504.	0.3	5
75	Structural and electrical properties of high-quality 0.41μm-thick InSb films grown on GaAs (100) substrate with InxAl1â^xSb continuously graded buffer. Materials Research Bulletin, 2012, 47, 2927-2930.	2.7	8
76	Single Crystalline β-Ag ₂ Te Nanowire as a New Topological Insulator. Nano Letters, 2012, 12, 4194-4199.	4.5	75
77	Quantum well thickness dependence of Rashba spin–orbit coupling in the InAs/InGaAs heterostructure. Applied Physics Letters, 2011, 98, 202504.	1.5	14
78	Injection, detection and gate voltage control of spins in the spin field effect transistor. Journal of Applied Physics, 2011, 109, 102405.	1.1	6
79	Detection of Rashba field using a rotational applied field. Journal of Applied Physics, 2011, 109, 07C313.	1.1	2
80	A Case of Intrapancreatic Accessory Spleen Mistaken as a Pancreatic Mass due to Different Enhancing Pattern from Normal Spleen. Korean journal of gastroenterology = Taehan Sohwagi Hakhoe chi, The, 2011, 58, 357.	0.2	4
81	High mobility in a two dimensional electron system with a thinned barrier. Solid State Communications, 2011, 151, 1599-1601.	0.9	3
82	Rashba effect induced magnetoresistance in an InAs heterostructure. Thin Solid Films, 2011, 519, 8203-8206.	0.8	2
83	Crystalline anisotropy effect on magnetic properties and its competition with shape anisotropy. Metals and Materials International, 2011, 17, 509-513.	1.8	2
84	Nonlocal voltage in a spin field effect transistor with finite channel width. Current Applied Physics, 2011, 11, 276-279.	1.1	1
85	Gate modulation of spin precession in a semiconductor channel. Journal Physics D: Applied Physics, 2011, 44, 064006.	1.3	9
86	Observation of Spin-Orbit Interaction Parameter Over a Wide Temperature Range Using Potentiometric Measurement. IEEE Transactions on Magnetics, 2010, 46, 1562-1564.	1.2	10
87	Electronic phase coherence and relaxation in graphene field effect transistor. Solid State Communications, 2010, 150, 1987-1990.	0.9	14
88	Spin-orbit coupling in double-sided doped InAs quantum well structures. Applied Physics Letters, 2010, 97, 012504.	1.5	19
89	Manipulation of the Rashba Spin-orbit Interaction in Double-sided doped In0.53Ga0.47As/InAs Quantum-well Structures. Journal of the Korean Physical Society, 2010, 57, 1946-1949.	0.3	1
90	Influence of the Magnetic Field on the Effective Mass and the Rashba effect in an In0.53Ga0.47As Quantum-well Structure. Journal of the Korean Physical Society, 2010, 57, 1929-1932.	0.3	3

#	Article	IF	CITATIONS
91	Determination of Spin-Orbit Interaction in InAs Heterostructure. IEEE Transactions on Magnetics, 2009, 45, 2383-2385.	1.2	2
92	Spin Interaction Effect on Potentiometric Measurements in a Quantum Well Channel. IEEE Transactions on Magnetics, 2009, 45, 2389-2392.	1.2	1
93	A spin field effect transistor using stray magnetic fields. Solid-State Electronics, 2009, 53, 1016-1019.	0.8	4
94	Temperature dependence of spin injection efficiency in an epitaxially grown Fe/GaAs hybrid structure. Journal of Magnetism and Magnetic Materials, 2009, 321, 3795-3798.	1.0	5
95	Control of Spin Precession in a Spin-Injected Field Effect Transistor. Science, 2009, 325, 1515-1518.	6.0	491
96	Spin Transport in a Submicron-sized Structure Using Vanadium Metal Masks. Journal of the Korean Physical Society, 2009, 55, 207-211.	0.3	0
97	Interface resistance dependence of spin transport in a ferromagnet–semiconductor hybrid structure. Journal of Magnetism and Magnetic Materials, 2008, 320, 1436-1439.	1.0	7
98	Bistable Voltage Transition Using Spin-Orbit Interaction in a Ferromagnet-Semiconductor Hybrid Structure. IEEE Transactions on Magnetics, 2008, 44, 419-422.	1.2	1
99	Electric Field Effect on Spin Diffusion in a Semiconductor Channel. IEEE Transactions on Magnetics, 2008, 44, 2647-2650.	1.2	2
100	Spin Hall Effect Induced by a Pd/CoFe Multilayer in a Semiconductor Channel. Journal of the Korean Physical Society, 2008, 53, 1357-1362.	0.3	2
101	Influence of Growth Temperature on the Magnetic Anisotropy of Co Grown on GaAs (001) Substrates. Journal of the Korean Physical Society, 2008, 53, 3352-3355.	0.3	0
102	Channel width effect on the spin-orbit interaction parameter in a two-dimensional electron gas. Applied Physics Letters, 2007, 90, 112505.	1.5	33
103	Electrical spin injection and detection in an InAs quantum well. Applied Physics Letters, 2007, 90, 022101.	1.5	82
104	Effect of ferromagnetic nanoparticles on the transport properties of a GaMnAs microbridge. Applied Physics Letters, 2007, 91, 062513.	1.5	6
105	Magnetization reversal of ferromagnetic nanoparticles under inhomogeneous magnetic field. Journal of Magnetism and Magnetic Materials, 2007, 309, 272-277.	1.0	16
106	Unbalanced spin accumulation induced by spin Hall effect. Journal of Magnetism and Magnetic Materials, 2007, 310, e705-e707.	1.0	1
107	Resistance modulation using amperian field in a two-dimensional electron gas system. Journal of Magnetism and Magnetic Materials, 2007, 310, 1952-1954.	1.0	0
108	Spin-filtering effect in a two-dimensional electron gas under a local fringe field. Physica Status Solidi (A) Applications and Materials Science, 2007, 204, 3958-3961.	0.8	1

#	ARTICLE	IF	CITATIONS
109	Inhomogeneous spin accumulation in Py/Au/Py spin valve. Physica Status Solidi (B): Basic Research, 2007, 244, 4530-4533.	0.7	2
110	Observation of room temperature magnetoresistance in a lateral ferromagnet–semiconductor structure. Physica Status Solidi (B): Basic Research, 2007, 244, 4448-4451.	0.7	0
111	Transport property of insulating barrier in a ferromagnet-semiconductor hybrid system. Solid-State Electronics, 2006, 50, 1682-1686.	0.8	0
112	Spin hall effect in an inverted heterostructure. , 2006, , .		0
113	Spin transport in an InAs based two-dimensional electron gas nanochannel. Journal of Applied Physics, 2005, 97, 10D502.	1.1	1
114	A New Reference Signal Generation Method for MRAM Using a 90-Degree Rotated MTJ. IEEE Transactions on Magnetics, 2004, 40, 2628-2630.	1.2	2
115	Influence of annealing on Co/Au multilayers: a structural and magnetic study. Thin Solid Films, 2003, 428, 102-106.	0.8	16
116	Dependence of the perpendicular anisotropy in Co/Au multilayers on the number of repetitions. Journal of Applied Physics, 2003, 93, 7241-7243.	1.1	12
117	Current-controlled bi-stable domain configurations in Ni81Fe19 elements: An approach to magnetic memory devices. Applied Physics Letters, 2002, 81, 862-864.	1.5	51
118	Magnetic properties of perpendicularly magnetized Co/Au multilayers. Journal of Magnetism and Magnetic Materials, 2002, 240, 526-528.	1.0	13
119	Investigation of the magnetic interaction of small Permalloy particles. IEEE Transactions on Magnetics, 2001, 37, 2049-2051.	1.2	5
120	Properties of lithographically formed cobalt and cobalt alloy single crystal patterned media. IEEE Transactions on Magnetics, 2000, 36, 2987-2989.	1.2	12
121	Detection and Control of the Effective Magnetic Field in a Caâ€Doped Bi 2 Se 3 Topological Insulator. Advanced Electronic Materials, 0, , 2101075.	2.6	0